Journal of Theoretical and Applied Information Technology
20th February 2013. Vol. 48 No.2

ISSN: 1992-8645 www.jatit.org E-ISSN: 1817-3195

ANALYSIS ON DYNAMIC ELASTIC MODULUS AND DISSIPATION FACTOR OF POROUS MEDIUM

[1,2] WENHAI HE

[1] School of Mechanical Engineering, Xi'an Jiaotong University, Xi'an 710049, Shannxi, China
[2] College of Mechanical Engineering, Xi'an University of Science and Technology, Xi'an 710054, Shannxi, China

ABSTRACT

Open-celled porous medium which has conspicuous damping characteristic is useful to control noise and vibration. This medium is composed of two phases, namely solid matrix and entrapped fluid. The inertia of these two phases and the interaction between them are taken into account for developing its dynamic elastic modulus and dissipation factor. Simulation shows that the dynamic elastic modulus is complex number, and its real part and image part depend on frequency. For single-layer open-celled porous medium, the image part is not monotonous and reaches peak at a certain frequency. But the real part increases monotonously with frequency. So, its dissipation factor also has one peak at the certain frequency. In low and high frequency ranges, its dissipation factor is very small. For two-layer open-celled porous medium, its dissipation factor has two peaks in low and high frequency ranges, respectively. And, two peak frequencies decrease with the increasing of total thickness of porous medium. In comparison with signal-layer open-celled porous medium, the two-layer one is more available to control noise and vibration in high frequency range.

Keywords: *Dynamic Elastic Modulus, Dissipation Factor, Porous Medium, Boundary Condition, Continuity Condition*

1. INTRODUCTION

Open-celled porous medium is widely used as ideal material for absorbing noise and reducing vibration [1]. This kind of material is composed of solid matrix and entrapped fluid in pores embedded in the matrix. Golovin et al. [2] revealed that open-celled porous medium has conspicuous energy dissipation and damping characteristics. Energy dissipation of this medium arises from relative motion and interaction between the solid matrix and the entrapped fluid [3]. Dissipation factor can reveal obviously its damping. Okuno et al. [4] had developed the damping of open-celled porous medium, but they assumed that porous medium was quasi-static. So, the inertia of solid matrix and entrapped fluid are neglected. Wijesinghe et al. [5] assumed open-celled porous medium is non-dissipation. So, the interaction between solid matrix and entrapped fluid is also neglected.

In previous works, open-celled porous medium is single-layer. Practices prove that multilayered open-celled porous medium has more superiority. So, it is necessary to develop the damping characteristic of multilayered open-celled porous material for its rational application.

In this paper, dynamic elastic modulus and dissipation factor of single-layer and two-layer open-celled porous media are researched. The inertia of two phases and the interaction between them both are taken fully into account.

2. STRESS AND DEFORMATION OF SINGLE-LAYER OPEN-CELLED POROUS MEDIUM

Single-layer open-celled porous medium which is excited by distributed loading on its top is shown in Figure 1.

This paper focuses on the open-celled porous medium which is excited by low loading, such as sound pressure. So, the deformation of its solid matrix is in linear elastic range. Otherwise, the entrapped fluid belongs to viscous Newtonian fluid.

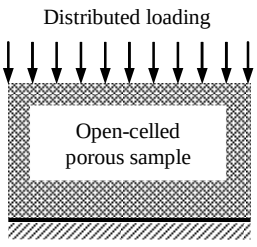

Figure 1: Signal-Layer Open-Celled Porous Medium Under Distributed Loading

ISSN: 1992-8645 www.jatit.org E-ISSN: 1817-3195

2.1 Mechanical Model Of Open-Celled Porous Medium

It is known from Biot [6, 7] that the dynamics equations of open-celled porous medium satisfy

$$\frac{\partial \sigma_x}{\partial x}+\frac{\partial \tau_{xy}}{\partial y}+\frac{\partial \tau_{xz}}{\partial z}+\rho\frac{\partial^2 u}{\partial t^2}+\rho_f\frac{\partial^2 w_x}{\partial t^2}+\frac{\partial P}{\partial x}=0 \quad (1)$$

$$\frac{\partial \tau_{yx}}{\partial x}+\frac{\partial \sigma_y}{\partial y}+\frac{\partial \tau_{yz}}{\partial z}+\rho\frac{\partial^2 v}{\partial t^2}+\rho_f\frac{\partial^2 w_y}{\partial t^2}+\frac{\partial P}{\partial y}=0 \quad (2)$$

$$\frac{\partial \tau_{xz}}{\partial x}+\frac{\partial \tau_{zy}}{\partial y}+\frac{\partial \sigma_z}{\partial z}+\rho\frac{\partial^2 w}{\partial t^2}+\rho_f\frac{\partial^2 w_z}{\partial t^2}+\frac{\partial P}{\partial z}=0 \quad (3)$$

Where σ_m and τ_{mn} are normal and shear stress of solid matrix in x, y and z direction. m and n represent x, y and z. u, v and w are displacements of solid matrix in three directions. w_x, w_y and w_z are relative displacement between solid matrix and entrapped fluid in three directions. P and ρ_f are pressure and mass density of the entrapped fluid, respectively. ρ is mass density of the solid matrix.

During the solid matrix deforming, the entrapped fluid which is Newtonian fluid flows in interlinked pores. And, the seepage equation satisfies

$$\frac{\partial^2 w_x}{\partial x\partial t}+\frac{\partial^2 w_y}{\partial y\partial t}+\frac{\partial^2 w_z}{\partial z\partial t}=-\left[\frac{\partial^2 u}{\partial x\partial t}+\frac{\partial^2 v}{\partial y\partial t}+\frac{\partial^2 w}{\partial z\partial t}\right] \quad (4)$$

where t is time.

In linear elastic range, it is known from Hooker's law that the normal stresses of the solid matrix satisfy

$$\sigma_x=-\frac{2}{1-2\nu}\left[G(1-\nu)\frac{\partial u}{\partial x}+G\nu\left[\frac{\partial v}{\partial y}+\frac{\partial w}{\partial z}\right]\right] \quad (5)$$

$$\sigma_y=-\frac{2}{1-2\nu}\left[G(1-\nu)\frac{\partial v}{\partial y}+G\nu\left[\frac{\partial u}{\partial x}+\frac{\partial w}{\partial z}\right]\right] \quad (6)$$

$$\sigma_z=-\frac{2}{1-2\nu}\left[G(1-\nu)\frac{\partial w}{\partial z}+G\nu\left[\frac{\partial v}{\partial y}+\frac{\partial u}{\partial x}\right]\right] \quad (7)$$

where G and ν are the shear modulus and Poisson ratio of the solid matrix, respectively.

According to Darcy's law, the dynamic seepage of the entrapped fluid in open-celled porous medium satisfy

$$\frac{\partial P}{\partial x}=-\rho_f\left[\frac{g}{K_d}\frac{\partial w_x}{\partial t}+\frac{\partial^2 u}{\partial t^2}+\frac{1}{\phi}\frac{\partial^2 w_x}{\partial t^2}\right] \quad (8)$$

$$\frac{\partial P}{\partial y}=-\rho_f\left[\frac{g}{K_d}\frac{\partial w_y}{\partial t}+\frac{\partial^2 v}{\partial t^2}+\frac{1}{\phi}\frac{\partial^2 w_y}{\partial t^2}\right] \quad (9)$$

$$\frac{\partial P}{\partial z}=-\rho_f\left[\frac{g}{K_d}\frac{\partial w_z}{\partial t}+\frac{\partial^2 w}{\partial t^2}+\frac{1}{\phi}\frac{\partial^2 w_z}{\partial t^2}\right] \quad (10)$$

Where K_d and ϕ are the permeability and porosity of open-celled porous medium, respectively.

It is assumed that the open-celled porous medium shown in Figure 1 is excited by distributed loading whose frequency is ω. So, the steady state response of the porous medium to this loading satisfies

$$\varpi(x,y,z,t)=\overline{\varpi}(x,y,z)\exp(i\omega t) \quad (11)$$

where ϖ represents u, v, w, u_f, v_f, w_f, w_x, w_y, w_z, P, σ_m and τ_{mn}. u_f, v_f and w_f are average displacement of the entrapped fluid, respectively. $\overline{\varpi}$ represents the amplitudes of above parameters, namely $\overline{u}$, $\overline{v}$, $\overline{w}$, $\overline{u}_f$, $\overline{v}_f$, $\overline{w}_f$, $\overline{w}_x$, $\overline{w}_y$, $\overline{w}_z$, $\overline{P}$, $\overline{\sigma}_m$ and $\overline{\tau}_{mn}$. i is imaginary unit.

Substituting Eq. (11) into Eq. (8), (9) and (10), yield

$$\frac{\partial \overline{P}}{\partial x}=-\rho_f\left[\frac{ig\overline{w}_x\omega}{K_d}-\overline{u}\omega^2-\frac{\overline{w}_x\omega^2}{\phi}\right] \quad (12)$$

$$\frac{\partial \overline{P}}{\partial y}=-\rho_f\left[\frac{ig\overline{w}_y\omega}{K_d}-\overline{v}\omega^2-\frac{\overline{w}_y\omega^2}{\phi}\right] \quad (13)$$

$$\frac{\partial \overline{P}}{\partial z}=-\rho_f\left[\frac{ig\overline{w}_z\omega}{K_d}-\overline{w}\omega^2-\frac{\overline{w}_z\omega^2}{\phi}\right] \quad (14)$$

The relative displacement between the solid matrix and the entrapped fluid can be obtained based on above analysis, and they satisfy

$$\overline{w}_x=\frac{c}{\rho_f\omega^2}\left[\rho_f\omega^2\overline{u}-\frac{\partial \overline{P}}{\partial x}\right] \quad (15)$$

ISSN: 1992-8645 www.jatit.org E-ISSN: 1817-3195

$$\overline{w}_y = \frac{c}{\rho_f \omega^2}\left[\rho_f \omega^2 \overline{v} - \frac{\partial \overline{P}}{\partial y}\right] \quad (16)$$

$$\overline{w}_z = \frac{c}{\rho_f \omega^2}\left[\rho_f \omega^2 \overline{w} - \frac{\partial \overline{P}}{\partial z}\right] \quad (17)$$

where $c = K_d \phi\omega/(g\phi i - K_d\omega)$.

Substituting Eq. (5), (6), (7) and (11) into Eq. (1), yield

$$\begin{aligned}&\Lambda\frac{\partial^2\overline{u}}{\partial x^2} - G\frac{\partial^2\overline{u}}{\partial y^2} - G\frac{\partial^2\overline{u}}{\partial z^2} + (\Pi - G)\frac{\partial^2\overline{v}}{\partial x\partial y}\\ &+ (\Pi - G)\frac{\partial^2\overline{w}}{\partial x\partial z} = \omega^2\rho\overline{u} + \omega^2\rho_f\overline{w}_x - \frac{\partial\overline{P}}{\partial x}\end{aligned} \quad (18)$$

$$\begin{aligned}&-G\frac{\partial^2\overline{v}}{\partial^2 x} + \Lambda\frac{\partial^2\overline{v}}{\partial y^2} - G\frac{\partial^2\overline{v}}{\partial z^2} + (\Pi - G)\frac{\partial^2\overline{u}}{\partial x\partial y}\\ &+ (\Pi - G)\frac{\partial^2\overline{w}}{\partial y\partial z} = \omega^2\rho\overline{v} + \omega^2\rho_f\overline{w}_y - \frac{\partial\overline{P}}{\partial y}\end{aligned} \quad (19)$$

$$\begin{aligned}&-G\frac{\partial^2\overline{w}}{\partial x^2} - G\frac{\partial^2\overline{w}}{\partial y^2} + \Lambda\frac{\partial^2\overline{w}}{\partial z^2} + (\Pi - G)\frac{\partial^2\overline{u}}{\partial x\partial z}\\ &+ (\Pi - G)\frac{\partial^2\overline{v}}{\partial y\partial z} = \omega^2\rho\overline{w} + \omega^2\rho_f\overline{w}_z - \frac{\partial\overline{P}}{\partial z}\end{aligned} \quad (20)$$

where $\Lambda = -\dfrac{E(1-\nu)}{(1+\nu)(1-2\nu)}$,

$\Pi = -\dfrac{E\nu}{(1+\nu)(1-2\nu)}$.

Substituting Eq. (8), (9) and (10) into Eq. (18), (19) and (20), yield

$$\begin{aligned}&\Lambda\frac{\partial^2\overline{u}}{\partial x^2} - G\frac{\partial^2\overline{u}}{\partial y^2} - G\frac{\partial^2\overline{u}}{\partial z^2} + (\Pi - G)\frac{\partial^2\overline{v}}{\partial x\partial y}\\ &+ (\Pi - G)\frac{\partial^2\overline{w}}{\partial x\partial z} = (\rho + c\rho_f)\omega^2\overline{u} - (1+c)\frac{\partial\overline{P}}{\partial x}\end{aligned} \quad (21)$$

$$\begin{aligned}&-G\frac{\partial^2\overline{v}}{\partial^2 x} + \Lambda\frac{\partial^2\overline{v}}{\partial y^2} - G\frac{\partial^2\overline{v}}{\partial z^2} + (\Pi - G)\frac{\partial^2\overline{u}}{\partial x\partial y}\\ &+ (\Pi - G)\frac{\partial^2\overline{w}}{\partial y\partial z} = (\rho + c\rho_f)\omega^2\overline{v} - (1+c)\frac{\partial\overline{P}}{\partial y}\end{aligned} \quad (22)$$

$$\begin{aligned}&-G\frac{\partial^2\overline{w}}{\partial x^2} - G\frac{\partial^2\overline{w}}{\partial y^2} + \Lambda\frac{\partial^2\overline{w}}{\partial z^2} + (\Pi - G)\frac{\partial^2\overline{u}}{\partial x\partial z}\\ &+ (\Pi - G)\frac{\partial^2\overline{v}}{\partial y\partial z} = (\rho + c\rho_f)\omega^2\overline{u} - (1+c)\frac{\partial\overline{P}}{\partial z}\end{aligned} \quad (23)$$

Fourier transform is used in the present paper for solving partial differential equations. The definition of Fourier transform is

$$f^*(\xi,\eta) = \int_{-\infty}^{+\infty}\int_{-\infty}^{+\infty} f(x,y)e^{-i(\xi x+\eta y)}dxdy \quad (24)$$

Equation (21), (22) and (23) are transformed into Fourier domain according to the definition of Fourier transform.

$$\begin{aligned}&-G\frac{\partial^2\overline{u}^*}{\partial z^2} + i\xi(\Pi - G)\frac{\partial\overline{w}^*}{\partial z}\\ &+[G\eta^2 - \Lambda\xi^2 - (\rho + c\rho_f)\omega^2]\overline{u}^*\\ &-(\Pi - G)\xi\eta\overline{v}^* + i\xi(1+c)\overline{P}^* = 0\end{aligned} \quad (25)$$

$$\begin{aligned}&-G\frac{\partial^2\overline{v}^*}{\partial z^2} + i\eta(\Pi - G)\frac{\partial\overline{w}^*}{\partial z}\\ &+[G\xi^2 - \Lambda\eta^2 - (\rho + c\rho_f)\omega^2]\overline{v}^*\\ &-(\Pi - G)\xi\eta\overline{u}^* + i\eta(1+c)\overline{P}^* = 0\end{aligned} \quad (26)$$

$$\begin{aligned}&\Lambda\frac{\partial^2\overline{w}^*}{\partial z} + i\xi(\Pi - G)\frac{\partial\overline{u}^*}{\partial z}\\ &+i\eta\,(\Pi - G)\frac{\partial\overline{v}^*}{\partial z}\\ &+[G\xi^2 + G\eta^2 - (\rho + c\rho_f)\omega^2]\overline{w}^*\\ &+(1+c)\frac{\partial\overline{P}^*}{\partial z} = 0\end{aligned} \quad (27)$$

It can be obtained from Eq. (4), (15), (16) and (17) that

$$\begin{aligned}&\frac{c}{\rho_f w^2}\left[\frac{\partial^2\overline{P}}{\partial x^2} + \frac{\partial^2\overline{P}}{\partial y^2} + \frac{\partial^2\overline{P}}{\partial z^2}\right]\\ &= (1+c)\left[\frac{\partial\overline{u}}{\partial x} + \frac{\partial\overline{v}}{\partial y} + \frac{\partial\overline{w}}{\partial z}\right]\end{aligned} \quad (28)$$

According to the definition of Fourier transform, Eq. (28) is transformed into Fourier domain, yield

$$\begin{aligned}&-\frac{c}{\rho_f\omega^2}(\xi^2 + \eta^2)\overline{P}^* - c(i\xi\overline{u}^* + i\eta\overline{v}^*)\\ &+\frac{c}{\rho_f\omega^2}\left[\frac{\partial^2\overline{P}^*}{\partial z^2} - \rho_f\omega^2\frac{\partial\overline{w}^*}{\partial z}\right]\\ &= i\xi\overline{u}^* + i\eta\overline{v}^* + \frac{\partial\overline{w}^*}{\partial z}\end{aligned} \quad (29)$$

Under distributed loading, the volume strain of the solid matrix of the open-celled porous medium satisfies

ISSN: 1992-8645 www.jatit.org E-ISSN: 1817-3195

$$e = \frac{\partial u}{\partial x} + \frac{\partial v}{\partial y} + \frac{\partial w}{\partial z} \tag{30}$$

Because the frequency of loading is ω, it is known from Eq. (11) that the volume strain of the solid matrix satisfies

$$e = \bar{e}\exp(i\omega t) \tag{31}$$

Substituting Eq. (11) and (31) into Eq. (30), yield

$$\bar{e} = \frac{\partial \bar{u}}{\partial x} + \frac{\partial \bar{v}}{\partial y} + \frac{\partial \bar{w}}{\partial z} \tag{32}$$

Equation (32) is transformed into Fourier domain based on the definition of Fourier transform shown in Eq. (24)

$$\bar{e}^* = i\xi\bar{u}^* + i\eta\bar{v}^* + \frac{\partial \bar{w}^*}{\partial z} \tag{33}$$

It is known from above analysis that there are five equations in Fourier domain, such as Eq. (25), (26), (27), (29) and (33). Five parameters, such as $\bar{u}^*$, $\bar{v}^*$, $\bar{w}^*$, $\bar{P}^*$ and $\bar{e}^*$ can be obtained.

Based on numerical inversion Fourier transform, the displacements of open-celled porous medium, such as u, v and w can be obtained. Substituting them into Eq. (5), (6) and (7), the normal stresses of the medium, such as σ_x, σ_y and σ_z can also be obtained.

In z direction, the dynamic elastic modulus satisfy

$$E = \frac{\sigma_z}{\varepsilon_z} \tag{34}$$

where ε_z is the strain.

It is known from above analysis that dynamic modulus is complex and depends on frequency, and the dissipation factor is

$$\eta = \mathrm{Im}(E)/\mathrm{Re}(E) \tag{35}$$

2.2 Structure Parameters Of Open-Celled Porous Medium

Zhu et al. [8] and Roberts et al. [9] concluded that static Young modulus and Poisson ration of the solid matrix are relative to its microstructure and its relative density. It is generally assumed that open-celled porous medium is composed of regular cells arranged periodically. So, the porous medium will be macro anisotropy. But the actual porous medium is isotropy. Zhu [10] revealed that the open-celled porous medium which is composed of tetradaidecaledral cells can exhibit relative low anisotropy, and approximate to actual open-celled porous medium. So, the tetradaidecaledral cell is a good model for representing the microstructure of open-celled porous medium. And this kind of cell exists in actual open-celled polyurethane, open-celled ceramics [11], and open-celled metal [12, 13].

Zhu et al. [8] developed the compressive deformation of high porosity open-celled porous medium, and they taken into account the stretching, bending and twisting mechanisms of the solid matrix. Static Young modulus satisfies

$$E_{static} = \frac{0.726E_sR^2}{1+1.09R} \tag{36}$$

where E_s is Young modulus of material from which the solid matrix is made.

The relative density of open-celled porous medium satisfies

$$R = 1 - \frac{\rho_f}{\rho} \tag{37}$$

It is known from Zhu et al. [8] that Poisson ration of open-celled porous medium is zero if the deformation of solid matrix is less than 12%.

3. TWO-LAYER OPEN-CELLED POROUS MEDIUM

Two open-celled porous blocks are piled up in z direction, so two-layer open-celled medium is shown in Figure 2. The thickness of these open-celled porous blocks are d_1 and d_2, respectively.

In Figure 2, the distributed loading acts on the top of the two-layer open-celled porous medium. And, the bottom of this medium is restricted rigidly.

3.1 Boundary Condition

It is known that the entrapped fluid is hermetical or permeable at the boundaries of open-celled porous medium.

At the bottom of the two-layer porous medium shown in Figure 2, the flux of the entrapped fluid is zero because the bottom is hermetical. According to Darcy's law, its boundary condition satisfies

$$\left.\frac{dP}{dz}\right|_{z=0} = 0 \tag{38}$$

In Figure 2, the top of the two-layer open-celled medium is permeable. The pressure of the

Journal of Theoretical and Applied Information Technology
20th February 2013. Vol. 48 No.2

ISSN: 1992-8645 www.jatit.org E-ISSN: 1817-3195

entrapped fluid at top is equal to p which is the pressure of environment air. The boundary condition at this surface satisfies

$$P\big|_{z=d_1+d_2} = p \tag{39}$$

At the bottom of the two-layer medium shown in Figure 2, the displacements of the medium in x and z direction is zero because it is restricted rigidly, the boundary condition satisfies

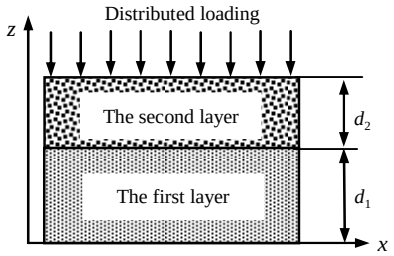

Figure 2: Schematic of two-layer open-celled porous medium under distributed loading

$$u\big|_{z=0} = 0 \tag{40}$$

$$w\big|_{z=0} = 0 \tag{41}$$

In Figure 2, the top is excited by distributed loading F .The shear stress on top is zero. So, its boundary condition satisfies

$$\sigma_z\big|_{z=d_1+d_2} = F \tag{42}$$

$$\tau_{xz}\big|_{z=d_1+d_2} = 0 \tag{43}$$

3.2 Continuity Condition

This paper focuses on high porosity open-celled porous medium, so the pores embedded in the solid matrix are interlinked at the interface of two open-celled porous blocks.

At the interface of two open-celled porous blocks shown in Figure 2, the normal and shear stresses of the solid matrix are equal. So, the continuity condition satisfies

$$\sigma_z^{(1)}\big|_{z=d_1} = \sigma_z^{(2)}\big|_{z=d_1} \tag{44}$$

$$\tau_{xz}^{(1)}\big|_{z=d_1} = \tau_{xz}^{(2)}\big|_{z=d_1} \tag{45}$$

At the interface of two open-celled porous blocks shown in Figure 2, the pressures of the entrapped fluid are equal, the continuity condition satisfies

$$P^{(1)}\big|_{z=d_1} = P^{(2)}\big|_{z=d_1} \tag{46}$$

At the interface of two open-celled porous blocks shown in Figure 2, the normal and tangential displacements of their solid matrixes are equal. So, the continuity condition satisfies

$$u^{(1)}\big|_{z=d_1} = u^{(2)}\big|_{z=d_1} \tag{47}$$

$$w^{(1)}\big|_{z=d_1} = w^{(2)}\big|_{z=d_1} \tag{48}$$

At the interface of two open-celled porous blocks shown in Figure 2, the fluxes of the entrapped fluid are equal, so the boundary condition satisfies

$$\frac{dP^{(1)}}{dz}\bigg|_{z=d_1} = \frac{dP^{(2)}}{dz}\bigg|_{z=d_1} \tag{49}$$

4. SIMULATION

In the present paper, two kinds of open-celled porous media are used for simulation. Static Young modulus of material from which their solid matrixes is made is 100 GPa. The entrapped fluid is air, and its dynamic viscosity and bulk modulus are 1.79×10^{-5} N·s/m^2 and 1.49×10^5 N/m^2, respectively.

4.1 Dynamic Elastic Modulus Of Open-Celled Porous Medium

It is known from above analysis that the dynamic elastic modulus is complex number and depends on frequency.

The porosities of open-celled porous media are 75%, 85% and 95%, respectively. And, their thicknesses are all 0.035m. Figure 3 shows that image parts of dynamic elastic modulus of three porous media are not monotonous, and their peaks are equal. But the peak frequencies increase with the increasing of porosity. The real parts of dynamic elastic modulus increase monotonously with the increasing of frequency.

If the porosities of three open-celled porous media are 85%, their thicknesses are 0.025m, 0.035m and 0.045m, respectively. Figure 4 shows that image parts of dynamic elastic modulus are not monotonous, and their peaks are equal. But the peak frequencies decrease with the increasing of thickness. The real parts of dynamic elastic modulus increase monotonoously with the increasing of frequency and thickness.

4.2 Dissipation Factor Of Open-Celled Porous Medium

An open-celled porous medium is excited by harmonic loading at its top which is permeable. It is

Journal of Theoretical and Applied Information Technology
20th February 2013. Vol. 48 No.2

ISSN: 1992-8645 www.jatit.org E-ISSN: 1817-3195

assumed that its bottom satisfies two boundary conditions.

Boundary condition 1: the bottom is restricted rigidly and hermetical; boundary condition 2: the bottom is restricted rigidly and permeable.

Figure 5 shows that open-celled porous medium exhibits visco-elastic characteristic.

Its dissipation factor reaches peak at a certain frequency. If the bottom is hermetical, the peak and the peak frequency of dissipation factor are higher. The dissipation factor is low in high frequency range.

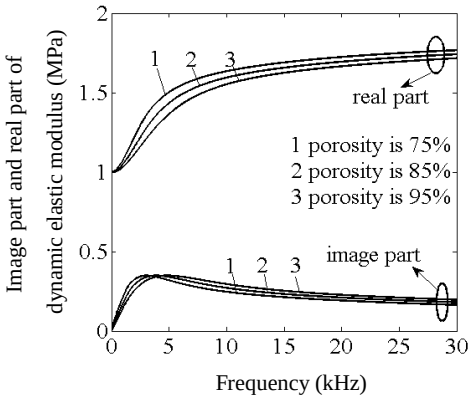

Figure 3: Image Part And Real Part Of Dynamic Elastic Modulus With Different Porosity

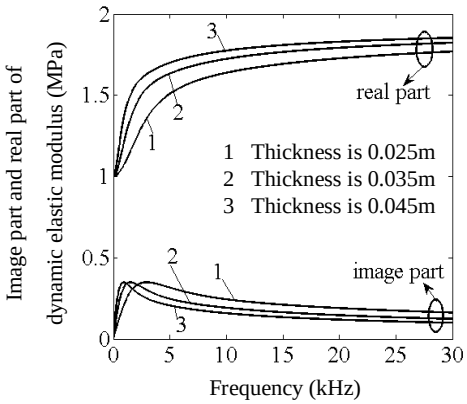

Figure 4: Image Part And Real Part Of Dynamic Elastic Modulus With Different Thickness

Two kinds of open-celled porous blocks are piled up. In this two-layer open-celled porous medium, the thickness and porosity of the first layer porous block are 0.030m and 95%, respectively. The porosity of the second layer porous block is 80%. It is assumed that the thicknesses of the second layer are 0.006m, 0.018m and 0.030m, respectively. So, there are three two-layer open-celled porous media whose total thicknesses are different. The dissipation factors of these media are shown in Figure 6.

Dissipation factor of two-layer open-celled porous medium has another peak at high frequency. So, it has higher damping in high frequency range.

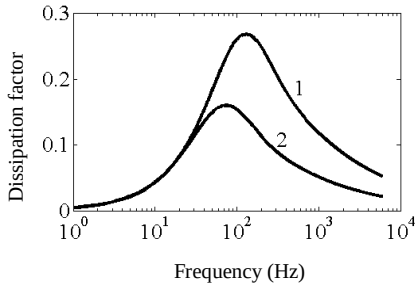

Figure 5: Dissipation Factor Of Signal Layer Open-Celled Porous Medium With Hermetical And Permeability Bottom

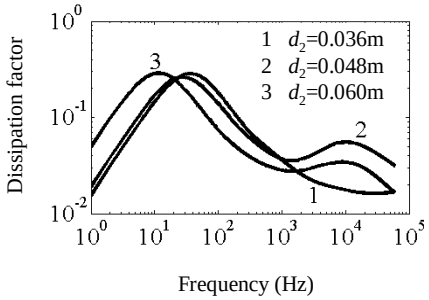

Figure 6: Dissipation Factor Of Two-Layer Porous Medium With Different Thickness Of The Second Layer

It is known from Figure 6 that two peak frequencies of the dissipation factor decrease with the increasing of total thickness of the two-layer open-celled porous medium.

5. CONCLUSIONS

Open-celled porous medium can exhibit visco-elasticity characteristic. Its dynamic elastic modulus is complex number and depends on frequency.

For signal-layer open-celled porous medium, it dissipation factor is not monotonous and reaches peak at a certain frequency. In low and high frequency ranges, the dissipation factor is small. And, the permeability of top and bottom can influence the dissipation factor. Peak and peak frequency of the dissipation factor of porous medium with hermetical bottom are higher than the one with permeable bottom.

ISSN: 1992-8645 www.jatit.org E-ISSN: 1817-3195

For two-layer open-celled porous medium, the dissipation factor has two peaks in low and high ranges respectively. Its peak frequencies decrease with the increasing of total thickness of the two-layer open-celled porous medium.

ACKNOWLEDGEMENT

This work is supported by 973 project (2006CB601204), Nature Science Foundation of China (51105302), and Scientific Research Program Funded by Shannxi Provincial Educational Department (11JK0879).

REFERENCES:

[1] Peter Goransson, "Acoustic and vibration damping in porous solids", *Philosophical Transactions Royal Society A*, Vol. 346, No. 1, 2006, pp. 89-108.

[2] I. S. Golovin, H. R. Sinning, "Damping in some cellular metallic materials", *Journal of Alloys and Compounds*, Vol. 355, No. 1, 2003, pp. 2-9.

[3] A. N. Gent, K. C. Rush, "Viscoelastic behavior of open-cell foams", *Rubber Chemical Technology*, Vol. 39, No. 1, 1966, pp. 10-15.

[4] A. Okuno, H. B. Kingsbury, "Dynamic modulus of poroelastic materials", *Journal of Applied Mechanics*, Vol. 56, No. 3, 1989, pp. 535-540.

[5] A. M. Wijesinghe, H. B. Kingsbury, "On the dynamic behavior of poroelastic materials", *Journal of the Acoustical Society of America*, Vol. 65, No. 1, 1979, pp. 90-95.

[6] M. A. Biot, "Theory of elastic wave propagation in a fluid saturated porous solid. Part I - low frequency range", *Journal of the Acoustical Society of America*, Vol. 28, No. 1, 1956, pp. 168-178.

[7] M. A. Biot, "Theory of elastic wave propagation in a fluid saturated porous solid. Part II - high frequency range" *Journal of the Acoustical Society of America*, Vol. 28, No. 1, 1956, pp. 179-191.

[8] H. X. Zhu, J. F. Knott, N. J. Mills, "Analysis of the elastic properties of open-cell foams with Tetrakaidecahedral Cells", *Journal of Mechanics and Physics Solids*, Vol. 45, No. 3, 1997, pp. 319 – 343.

[9] A. P. Robertsa and E. J. Garboczia, "Elastic properties of model random three-dimensional open-cell solids", *Journal of the Mechanics and Physics of Solids*, Vol. 50, No. 1, 2002, pp. 33-55.

[10] H. X. Zhu, N. J. Mills, J. F. Knott, "Analysis of the high strain compression of open-cell foams", *Journal of Mechanics and Physics Solids*, Vol. 45, No. 1, 1997, pp. 1875-1904.

[11] E. A. Moreira, M. D. M. Innocentini, J. R. Coury, "Permeability of eramic foams to compressible and in compressible flow", *Journal of the European Ceramic Society*, Vol. 24, No. 12, 2004, pp. 3209 – 3218.

[12] Jean-Francois Despois, Andreas Mortensen, "Permeability of open-pore microcellular materials", *Acta Materialia*, Vol. 53, No. 12, 2005, pp. 1381-1388.

[13] A. Bhattacharya, V. V. Calmidi, R. L. Mahajan, "Thermophysical properties of high porosity metal foams", *International Journal of Heat and Mass Transfer*, Vol. 45, No. 5, 2002, pp. 1017-1031.